Explainable Artificial Intelligence in Forecasting MT-InSAR Based Time Series Surface Movements

Nur Yagmur Aydin[1], Esra Erten[2], Gulsen Taskin[3], Nebiye Musaoglu[2]

[1] Gebze Technical University, Engineering Faculty, Geomatics Engineering Department, 41400, Kocaeli, Türkiye
[2] Istanbul Technical University, Civil Engineering Faculty, Geomatics Engineering Department, 34469, Istanbul, Türkiye
[3] Istanbul Technical University, Earthquake Engineering and Disaster Management Institute, 34469, Istanbul, Türkiye

Keywords: PSI, LSTM, Time Series Forecasting, Explainable Artificial Intelligence, SHAP.

Abstract

Explainable artificial intelligence (XAI) enables users to interpret the black box of machine learning (ML) algorithms and its applicability across various ML algorithms allows for the investigation of feature impacts on the model. Among the ML algorithms, Long Short Term Memory (LSTM) deep learning method has become popular in various applications, especially forecasting analysis, due to its ability to effectively capture long-range temporal dependencies in sequential data, as is often required when analyzing time-series deformation patterns derived from multi-temporal interferometric synthetic aperture radar (MT-InSAR). The SHapley Additive exPlanations (SHAP) method, one of the most popular XAI techniques, has been widely used to identify the impacts of features on processes. To this end, forecasting analysis of MT-InSAR-based time series surface movements was performed using the LSTM method in the two selected case regions at Istanbul Airport. These case regions exhibit different time series characteristics (subsidence and stable) and belong to different surface types (runway and building). According to the results obtained, the LSTM method showed successful performances with RMSE, MAE, and R values of 1.12 mm, 0.92 mm, 0.672 for case 1 and 1.37 mm, 1.13 mm, 0.385 for case 2. To assess the impacts of the exogenous variables, including trend, seasonal, and residual components of time series data and meteorological parameters gathered from the ERA5-Land dataset, were investigated using the SHAP method, and results were evaluated specifically for each case region.

1. Introduction

Deep learning (DL) neural networks have demonstrated successful applications; however, their non-linear and complex structures make them inherently non-interpretable (Kakogeorgiou et al., 2021). With the growing adoption of machine learning models, the need to explain these so-called “black box” models has become increasingly important. To address this challenge, explainable artificial intelligence (XAI) methods have been developed to interpret black-box decisions and enhance understanding of the machine learning model results. These methods enable the users and researchers to evaluate models with their explanations not only through accuracy metrics but also by providing meaningful explanations of the results (Ribeiro et al., 2016).

DL algorithms have been widely used in remote sensing applications such as classification (Kussul et al., 2017; Maxwell et al., 2018), soil moisture estimation (Celik et al., 2022; Huang et al., 2023), and forecasting (Rhif et al., 2020; Zhu et al., 2023). To enhance the interpretability of these models, methods such as LIME and SHAP (SHapley Additive exPlanations) have been developed and have increasingly gained a seat in remote sensing applications (Jena et al., 2023; Chen et al., 2023; Abdollahi and Pradhan, 2023). However, the use of XAI methods in forecasting studies remains limited (Lees et al., 2022; Zhang et al., 2023), particularly in the context of forecasting surface movement.

Forecasting of surface movements from the multi-temporal interferometric synthetic aperture radar (MT-InSAR) data has recently gained traction in the literature, with several studies conducted in mining areas (Hill et al., 2021), airports (Chen et al., 2021; Bayik and Abdikan, 2021; Bao et al., 2022), and urban environments (Liu et al., 2021). Yagmur et al. (2024) evaluated driving factors on time series forecasting of surface movements using permutation feature importance method. However, to date, no study has applied XAI methods to forecasting analysis, particularly in airport settings, which present complex trade-offs between economic development, transportation demands, and environmental conservation.

In this study, surface movement forecasting based on MT-InSAR analysis was conducted at Istanbul Airport using the Long Short-Term Memory (LSTM) DL method. The model was enhanced with exogenous variables, including trend, seasonal, and residual components of the time series, as well as meteorological parameters—air temperature, surface temperature, evaporation, and precipitation—obtained from ERA5-Land over the study area. The analysis focused on two case sites with distinct time series behaviours (subsidence and stable) and structural types. To interpret the influence of the exogenous variables, the SHAP method was applied to the forecasting results, which were then evaluated in relation to the time series characteristics and structural context of each site.

2. Study Area

Istanbul Airport is one of the largest airports in the world in terms of total area, located on the European side of Istanbul along the Black Sea coast. The vast area of 76.5 km^2 was allocated for its construction. Ground surveys began in 2014, and construction officially started in May 2015. The project was planned in four phases, with the first phase completed before the airport's official opening at the end of October 2018. Initially, the airport operated with two runways—Runways A

and B. Subsequently, Runway C was completed in June 2020, bringing the total number of runways to three, and the airport is scheduled for full completion in 2029.

Before the construction of the airport, the area had a long history of coal mining, industrial sand extraction, and clay deposits, dating back to the late 19th century. The open coal mines and excavation sites were eventually abandoned following a decline in coal consumption after the widespread adoption of natural gas in 1992. The land conversion for airport construction had significant environmental consequences, including the destruction of wetlands that had formed in the abandoned mining areas. The drainage and removal of these wetlands during construction likely resulted in habitat loss and ecosystem disruption (Yagmur et al., 2022). To create a level surface for construction, the drained wetlands were subsequently filled.

3. Data and Methodology

3.1 Data Used

The time series surface movement data for the study region were generated using Sentinel-1 Single Look Complex (SLC) satellite images, with the sensor specifications provided in Table 1. In the study, a total of 211 Sentinel-1 images, covering the period from November 5, 2018, to September 3, 2022, were processed using the SNAP and StaMPS software packages, with the master image dated June 15, 2020. The MT-InSAR processing followed the same methodology as described by Yagmur et al. (2022). The interferogram generation was carried out in SNAP software, while Persistent Scatterer Interferometry (PSI) analysis, which has been widely used in the deformation monitoring of structure (Halicioglu et al., 2021), was conducted in StaMPS through the following steps: phase noise estimation, persistent scatterer (PS) selection, PS weeding, phase correction, look angle error estimation, and atmospheric filtering, respectively.

Properties	Data
Track	58
Acquisition Mode	Ascending
Image Mode	Interferometric Wide
Wavelength	C band
Polarization	Vertical – Vertical (VV)
Spatial Resolution	5×20 m (range × azimuth)
Number of images	211
Temporal range	2018/11/05 - 2022/09/03
Master image	June 15, 2020

Table 1. The specifications of Sentinel-1 satellite images

Sentinel-1 satellite images have a spatial resolution of 5 × 20 meters in range and azimuth directions, respectively, and initially provided a temporal resolution of 6 days. However, following the failure of Sentinel-1B in mid-December 2021, data acquisition from this satellite ceased, resulting in a reduced temporal resolution of 12 days over Europe.

In this study, MT-InSAR deformation results served as inputs for forecasting surface movements and identifying the most influential exogenous features. These exogenous features were categorized into two groups: data-sourced features and meteorological features. The data-sourced features were derived by the decomposition of the time series surface movements into trend, seasonal, and residual components using an additional decomposition method. The meteorological features included air temperature (measured 2 meters above ground), surface temperature, precipitation, and evaporation, all obtained from ERA5-Land meteorological datasets.

The PSI-derived deformation results are presented in Fig. 1. The line-of-sight (LOS) deformation velocities range from -18.4 mm/year to 11.3 mm/year. The red and orange PS points indicate subsidence movements, while blue and green points represent uplift movements. Yellow points correspond to stable areas. For the time series forecasting analysis, two case regions with distinct deformation behaviours—one exhibiting subsidence and the other stability—were selected. These case regions are highlighted with black boxes in Fig. 1.

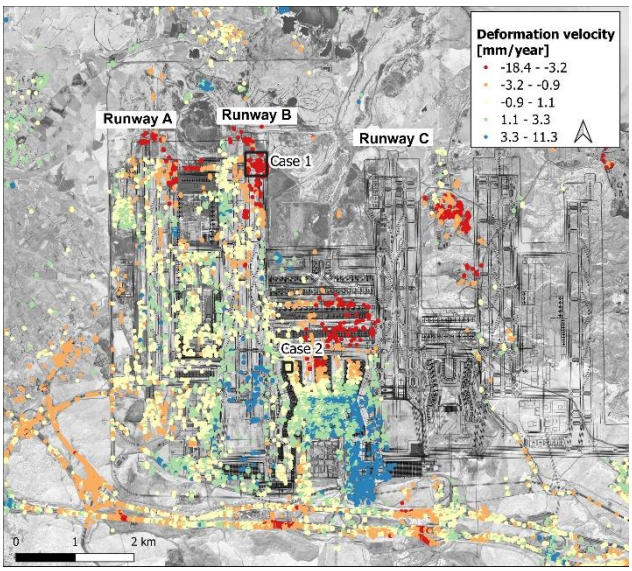

Figure 1. PSI deformation results of the Istanbul Airport.

3.2 Methodology

Prior to the forecasting analysis, data preparation steps were carried out. PS points within the selected regions were filtered based on a coherence threshold greater than 0.60. Subsequently, the weighted average of the time series surface movements for each region was calculated, with weights assigned according to the coherence values of the individual PS points. Due to the breakdown of the Sentinel-1B satellite in mid-December 2021, the temporal resolution of the dataset decreased from 6 days to 12 days. To maintain consistency and preserve a uniform 6-day interval, interpolation was performed for the affected period.

Following data preparation steps, forecasting analysis was conducted on the processed time series surface movement data for each case region. The time series data, covering the period from November 05, 2018 to September 03, 2022, were partitioned into training (85%) and testing (15%) subsets to ensure effective model training, hyperparameter tuning, and performance evaluation, respectively. The overall workflow of the study is illustrated in Fig. 2.

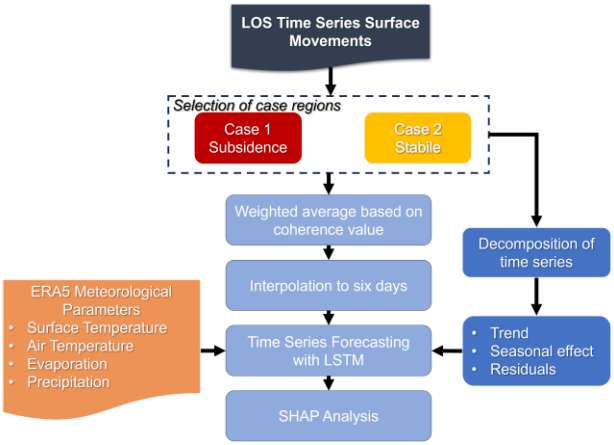

Figure 2. The flowchart of the study.

In the time series forecasting step, the LSTM method was applied to the LOS time series InSAR surface movements. Introduced by Hochreiter and Schmidhuber (1997), LSTM is a specialized type of recurrent neural network designed to effectively capture long-term dependencies in sequential data. It consists of three main components: memory cells, gates, and activation functions. The memory cell retains relevant information over long sequences, while the three gates—forget, input, and output—regulate the flow of information into and out of the cell. Activation functions control the updates and outputs of the memory cell, helping the network focus on important features (Liu et al., 2020). LSTM and its variants have become fundamental in deep learning for processing sequential data.

The accuracy assessment of the forecasting analysis was evaluated using three accuracy metrics: Root Mean Squared Error (RMSE), Mean Absolute Error (MAE), and the Pearson Correlation Coefficient (R) value. These metrics were calculated by comparing the forecasted values with the test data. The equations for each metric are provided below:

$$RMSE = \sqrt{\frac{\sum_{i=1}^{n}(x_i - \hat{x}_i)^2}{n}} \quad (1)$$

$$MAE = \frac{\sum_{i=1}^{n}|x_i - \hat{x}_i|}{n} \quad (2)$$

$$R = \frac{\sum_{i=1}^{n}(x_i - x_m)(\hat{x}_i - \hat{x}_m)}{\sqrt{\sum_{i=1}^{n}(x_i - x_m)^2 \sum_{i=1}^{n}(\hat{x}_i - \hat{x}_m)^2}} \quad (3)$$

where x_i is the measured value, $\hat{x}_i$ is the forecasted value, and n is the time step of the data. The x_m and $\hat{x}_m$ represent the average of measured and forecasted values, respectively.

To examine the influence of exogenous features—including trend, seasonal effect, residuals, and meteorological parameters (air temperature, surface temperature, evaporation, and precipitation)—on the forecasting of time series surface movements, the SHAP (SHapley Additive exPlanations) method was employed. SHAP is a robust tool for interpreting machine learning models, offering insights into the contribution of each input feature to the model's predictions. Developed by Lundberg and Lee (2017), SHAP values are based on cooperative game theory and the concept of Shapley values, ensuring a fair distribution of feature importance across predictions.

4. Results and Discussion

Forecasting analysis using the LSTM method was conducted with exogenous variables including components of the time series data and meteorological parameters. The accuracy results of the two cases are presented in Table 2. It is important to note that the test data were not used at any stage during model training, ensuring an unbiased evaluation of model performance.

Accuracy Metrics	Case 1	Case 2
RMSE (mm)	1.12	1.37
MAE (mm)	0.92	1.13
R	0.671	0.385

Table 2. Accuracy assessment results of forecasting analysis for two cases

According to Table 2, the RMSE and MAE values were found to be around 1 mm, indicating that the LSTM method effectively forecasted the test values. The model performed better in Case 1, with lower RMSE (1.12 mm) and MAE (0.92 mm) values and a higher correlation coefficient (R = 0.671), compared to Case 2, where R was lower (0.385) due to the nature of the stable time series.

The results obtained from the time series forecasting analysis are presented in Fig. 3. The green and red lines represent the training and test data, respectively. The black dashed line represents the LSTM forecast, which closely follows the test data, indicating that the model effectively learned and extended the trend. The LSTM model effectively captured the subsidence trend in Case 1 (Fig. 3a), while it demonstrated reasonable performance in tracking the stable pattern with minor fluctuations in Case 2 (Fig. 3b), despite the lower correlation coefficient. Overall, the LSTM model successfully captured the overall trends in both cases, as supported by the visual forecasting results.

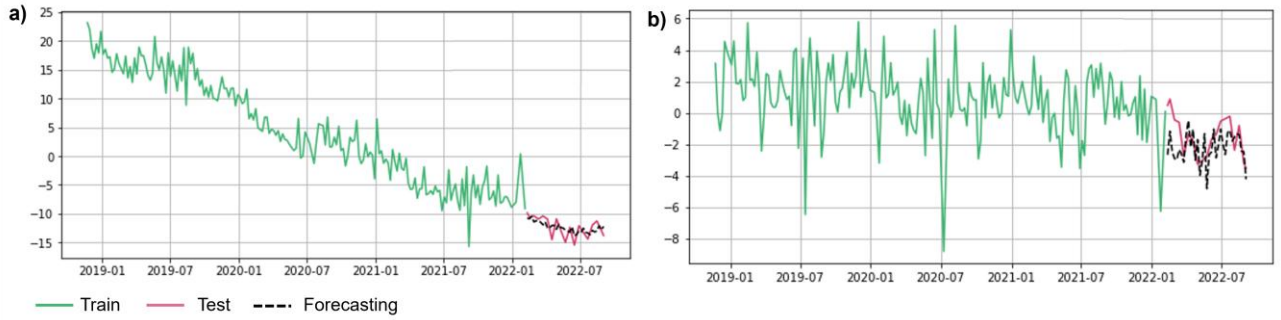

Figure 3. The forecasting results of a) Case 1 subsidence movement and b) Case 2 stable movement. The x-axis indicates the duration of the time series, and the y-axis indicates the LOS surface movements (mm).

To investigate the effects of exogenous variables on the forecasting of different time series patterns, the SHAP method was applied to both cases. Figure 4 presents the variables ranked by their impact values. In Case 1, which exhibits subsidence movement over Runway B, the trend component was identified as the most influential feature, followed by air temperature and surface temperature. In contrast, precipitation was found to have the least impact. In Case 2, representing a relatively stable region over the terminal building, the seasonal component was the most impactful, followed by surface temperature, evaporation, and the residual component. Notably, the trend had minimal influence in this case, likely due to the absence of a dominant long-term trend. Overall, these findings suggest that temperature-related and residual parameters are important in forecasting MT-InSAR-based surface movements, while the trend component plays a more significant role in areas exhibiting consistent deformation patterns, such as Case 1.

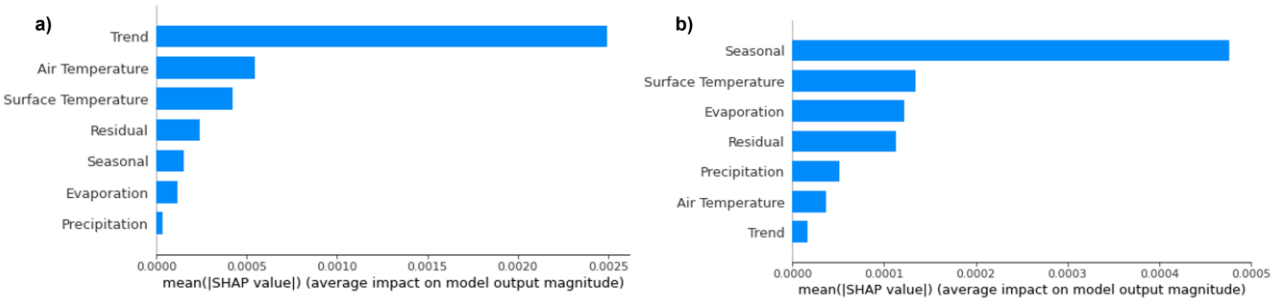

Figure 4. The forecasting results of a) Case 1 subsidence movement and b) Case 2 stable movement.

5. Conclusion

In this study, the influence of exogenous variables on the forecasting of time series with different characteristics was investigated. To this end, time series forecasting was conducted using the LSTM deep learning algorithm, and the contribution of exogenous variables to the forecasting performance was evaluated using the SHAP method. Both methods yielded promising results. The LSTM model successfully forecasted both time series with error values around 1 mm (RMSE and MAE). In Case 1, where a clear subsidence trend was observed, the trend component emerged as the most influential feature. In contrast, for Case 2, representing a more stable region, the seasonal component was found to be more prominent. Notably, surface temperature significantly influenced both time series, regardless of their differing temporal behaviors and structural contexts.

Overall, the findings emphasize the importance of identifying the key factors driving surface movements to enhance the reliability of forecasting models. Accurate forecasting of surface deformation is vital for early warning systems and risk mitigation, particularly in areas with critical infrastructure.

References

Abdollahi, A., Pradhan, B. (2023). Explainable artificial intelligence (XAI) for interpreting the contributing factors feed into the wildfire susceptibility prediction model. *Science of the Total Environment*, 879, 163004. doi.org/10.1016/j.scitotenv.2023.163004

Bao, X., Zhang, R., Shama, A., Li, S., Xie, L., Lv, J., ... Liu, G. (2022). Ground deformation pattern analysis and evolution prediction of Shanghai Pudong International Airport based on PSI long time series observations. *Remote sensing*, 14(3), 610. doi.org/10.3390/rs14030610

Bayik, C., Abdikan, S. (2021). Monitoring of small-scale deformation at sea-filled Ordu-Giresun Airport, Turkey from multi-temporal SAR data. *Engineering Failure Analysis*, 130, 105738, doi.org/10.1016/j.engfailanal.2021.105738.

Celik, M. F., Isik, M. S., Yuzugullu, O., Fajraoui, N., Erten, E. (2022). Soil moisture prediction from remote sensing images coupled with climate, soil texture and topography via deep learning. *Remote sensing*, 14(21), 5584. doi.org/10.3390/rs14215584

Chen, H., Yang, L., Wu, Q. (2023). Enhancing land cover mapping and monitoring: An interactive and explainable machine learning approach using Google Earth Engine. *Remote Sensing*, 15(18), 4585. doi.org/10.3390/rs15184585

Chen, Y., He, Y., Zhang, L., Chen, Y., Pu, H., Chen, B., Gao, L. (2021). Prediction of InSAR deformation time-series using a long short-term memory neural network. *International journal of remote sensing*, 42(18), 6919-6942. doi.org/10.1080/01431161.2021.1947540

Halicioglu, K., Erten, E., & Rossi, C. (2021). Monitoring deformations of Istanbul metro line stations through Sentinel-1 and levelling observations. Environmental Earth Sciences, 80(9), 361. doi.org/10.1007/s12665-021-09644-0

Hill, P., Biggs, J., Ponce-López, V., Bull, D. (2021). Time-series prediction approaches to forecasting deformation in Sentinel-1 INSAR data. *Journal of Geophysical Research: Solid Earth*, 126(3), e2020JB020176. doi.org/10.1029/2020JB020176

Hochreiter, S., Schmidhuber, J. (1997). Long short-term memory. *Neural computation*, 9(8), 1735-1780. doi.org/10.1162/neco.1997.9.8.1735

Huang, F., Zhang, Y., Zhang, Y., Shangguan, W., Li, Q., Li, L., Jiang, S. (2023). Interpreting Conv-LSTM for spatio-temporal soil moisture prediction in China. *Agriculture*, 13(5), 971. doi.org/10.3390/agriculture13050971

Jena, R., Shanableh, A., Al-Ruzouq, R., Pradhan, B., Gibril, M. B. A., Khalil, M. A., ... Ghamisi, P. (2023). Explainable artificial intelligence (XAI) model for earthquake spatial probability assessment in Arabian peninsula. *Remote Sensing*, 15(9), 2248. doi.org/10.3390/rs15092248

Kakogeorgiou, I., Karantzalos, K. (2021). Evaluating explainable artificial intelligence methods for multi-label deep learning classification tasks in remote sensing. *International Journal of Applied Earth Observation and Geoinformation*, 103, 102520. doi.org/10.1016/j.jag.2021.102520

Kussul, N., Lavreniuk, M., Skakun, S., Shelestov, A. (2017). Deep learning classification of land cover and crop types using remote sensing data. *IEEE Geoscience and Remote Sensing Letters*, 14(5), 778-782. doi.org/10.1109/LGRS.2017.2681128

Lees, T., Tseng, G., Atzberger, C., Reece, S., Dadson, S. (2022). Deep learning for vegetation health forecasting: a case study in Kenya. *Remote Sensing*, 14(3), 698. doi.org/10.3390/rs14030698

Liu, Q., Zhang, Y., Wei, J., Wu, H., Deng, M. (2021). HLSTM: Heterogeneous long short-term memory network for large-scale InSAR ground subsidence prediction. *IEEE Journal of Selected Topics in Applied Earth Observations and Remote Sensing*, 14, 8679-8688. doi.org/10.1109/JSTARS.2021.3106666

Liu, W., Pan, J., Ren, Y., Wu, Z., Wang, J. (2020). Coupling prediction model for long-term displacements of arch dams based on long short-term memory network. *Structural Control and Health Monitoring*, 27(7), e2548. doi.org/10.1002/stc.2548

Lundberg, S. M., Lee, S. I. (2017). A unified approach to interpreting model predictions. *Advances in neural information processing systems*, 30.

Maxwell, A. E., Warner, T. A., Fang, F. (2018). Implementation of machine-learning classification in remote sensing: An applied review. *International journal of remote sensing*, 39(9), 2784-2817. doi.org/10.1080/01431161.2018.1433343

Rhif, M., Ben Abbes, A., Martinez, B., Farah, I. R. (2020). A deep learning approach for forecasting non-stationary big remote sensing time series. *Arabian Journal of Geosciences*, 13(22), 1174. doi.org/10.1007/s12517-020-06140-w

Ribeiro, M. T., Singh, S., Guestrin, C. (2016). Explaining the predictions of any classifier. In Proceedings of the 22nd ACM SIGKDD International Conference on Knowledge Discovery and Data Mining, 1135-1144.

Yagmur, N., Erten, E., Musaoglu, N., Safak, E. (2022). Assessing spatio-temporal dynamics of large airport's surface stability. *Geocarto International*, 37(26), 13734-13747. doi.org/10.1080/10106049.2022.2082554

Yagmur, N., Taskin, G., Musaoglu, N., Erten, E. (2024). Forecasting surface movements based on PSI time series using machine learning algorithms. *International Journal of Remote Sensing*, 45(7), 2462-2485. doi.org/10.1080/01431161.2024.2331977

Zhang, Q., Li, P., Ren, X., Ning, J., Li, J., Liu, C., ... Wang, G. (2023). A new real-time groundwater level forecasting strategy: Coupling hybrid data-driven models with remote sensing data. *Journal of Hydrology*, 625, 129962. doi.org/10.1016/j.jhydrol.2023.129962

Zhu, S., Wei, J., Zhang, H., Xu, Y., Qin, H. (2023). Spatiotemporal deep learning rainfall-runoff forecasting combined with remote sensing precipitation products in large scale basins. *Journal of Hydrology*, 616, 128727. doi.org/10.1016/j.jhydrol.2022.128727